

Project: **1147**

Project title: **LAnd Management for CLimate Mitigation and Adaptation**

Principal investigator: **Julia Pongratz**

Report period: **2020-11-01 to 2021-08-31**

1. Overview

LAMACLIMA is a joint project with European Partners who use the project's DKRZ resources to run the MPI-ESM and collaboratively analyze results of two more Earth system models (Sec. 2-3) and process model output for applications in other model types (Sec. 4-5). Generally, within the LAMACLIMA project we investigate the effects of changed land cover and land management on climate (i.e. biogeophysical effects) and on biogeochemical cycles (in particular terrestrial emissions and uptake of CO₂). We focus on afforestation, cropland expansion, irrigation, and wood harvest to elaborate the effects of sustainable land-based adaptation and mitigation measures as potential negative emission technologies. Until now, the coupled nature of these effects overall receives limited consideration in land-use decision making processes. Here, we first investigate the local and remote biogeophysical and biogeochemical effects of the above-mentioned land cover and land management changes by Earth system model (ESM) sensitivity studies (MPI-ESM-1.2 was run on mistral, model output of MPI-ESM, CESM and EC-Earth is stored on /arch in order to ensure data exchange between all project partners). These results will be subsequently used by simulations with socio- and agro-economic models (so called integrated assessment models, IAMs) to identify their implications for the sectors of agriculture, forestry, and economic productivity including impacts on worker productivity. Finally, which is still work in progress, we design two contrary land cover and management scenarios within a series of Stakeholder Co-development workshops in order to complement the existing shared socioeconomic pathways (SSPs). These land-based climate mitigation scenarios, which should serve to achieve global net-zero emissions and thus the below 2°C climate goal, will then again be used within IAM and ESM simulations to study their socio-economic feasibility and coupled effects on the climate system.

2. Local biogeophysical effects of changed land cover and land management

Deforestation: The model results of the local temperature change due to deforestation are mostly within the observational range over all latitudes (see Fig. 1). Within the tropics, CESM simulates rather higher positive temperature change (+3°C) compared to MPI-ESM (+1°C), whereas in the northern mid-latitudes we find the opposite with -0.5°C for CESM and +1°C for MPI-ESM temperature change around 40°N. In northern high-latitudes, both models overestimate the observed cooling.

The energy balance decomposition shown in Fig. 1 is used to decompose the simulated impacts of land cover and land management changes on surface temperature to its underlying surface processes:

Cropland expansion (Fig. 1 a,b): The strongest cooling effect of albedo from cropland expansion is shown during Northern Hemisphere (NH) spring as a consequence of the reduced snow masking effect. The latent heat flux also contributes to a large part to the simulated temperature change, but in contrast to albedo with a positive impact. Overall MPI-ESM and CESM simulate a global warming of about 0.3 K over the year due to the local effect of cropland expansion.

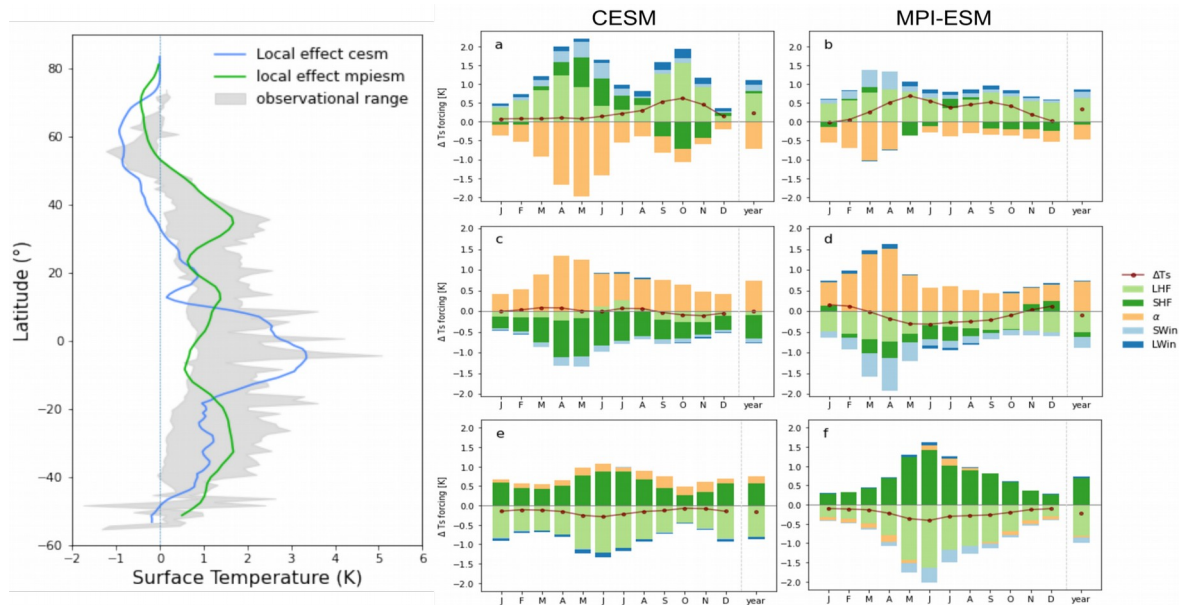


Figure 1: Left: Evaluation of local surface temperature effects from deforestation (derived from the cropland expansion and af-/reforestation simulations) with observational data (range in grey shade) from four estimates (Li et al., 2015; Alkama and Cescatti, 2016; Duveiller et al., 2018; Bright et al., 2017). Right: Seasonal energy balance decomposition of local surface temperature impact (a,b) for cropland expansion, (c,d) for af-/reforestation, and (e,f) for irrigation expansion, all for CESM and MPI-ESM, respectively.

Af-/reforestation (Fig. 1 c,d): The af-/reforestation-induced effect on albedo, which globally has a positive impact on the temperature has a clear seasonal peak during NH spring, similar to cropland expansion. The turbulent heat fluxes follow this intra-annual distribution with a distinct negative impact on surface temperature. This indicates that extratropical af-/reforestation is dominating on the global scale (not shown) with a strong albedo response counteracted by the turbulent heat fluxes. On average both models show a very low local temperature effect due to afforestation being quasi 0 K in CESM and -0.15 K in MPI-ESM.

Irrigation expansion (Fig. 1 e,f): The seasonal pattern is dominated by the dry season, when croplands are mostly irrigated. The strongest local cooling and subsequent turbulent heat fluxes are also simulated during NH spring and summer, as 2/3 of global land area is in the NH. This seasonal pattern is stronger in MPI-ESM as the irrigation extent reaches more northward than in CESM. On average, both models predict a slight cooling effect due to irrigation of around 0.2 K.

3. Unintended biogeochemical effects of changed land cover and land management

The above described biogeophysical effects can also have an impact on the remote climate, which in turn affects the biogeochemical cycle where no land cover or land management change occurred. Thus, we call it the unintended C cycle effect. Figure 2 shows these unintended effects on the total terrestrial carbon pool simulated by MPI-ESM1.2. Generally, the simulations show substantial unintended C losses and gains. The absolute negative impact on the land C pool from cropland expansion (-20 to -30 GtC, called *defrst* in Fig. 2) is higher compared to the absolute positive impact from af-/reforestation (+5 to +10 GtC). Additionally, the speed of declining land C pool is faster for cropland expansion than the C pool increase from af-/reforestation (quantification by

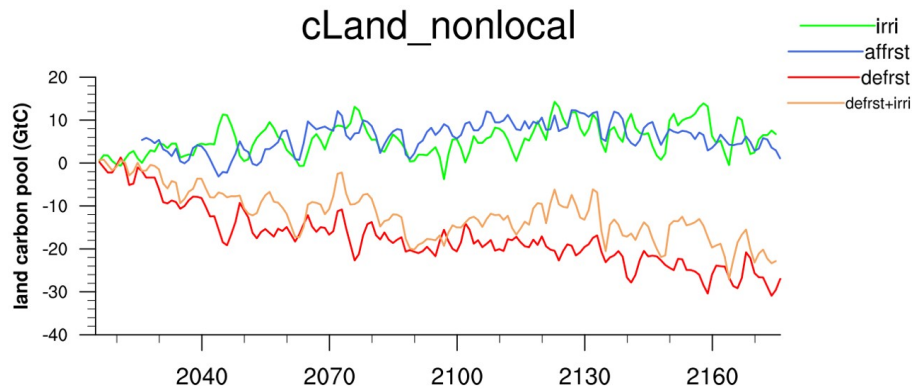


Figure 2: Unintended effects of irrigation, af-/reforestation, cropland expansion (defrst), and cropland expansion together with irrigation on total terrestrial carbon pool during a 160 year simulation period (year 2015 to 2175) under constant current environmental conditions.

time of emergence, not shown here). Interestingly, the simulation results indicate that the application of irrigation on croplands compared to no irrigation (often seen as a more "subtle" land use change than af-/reforestation) has an effect on additionally stored C via its remote climate effects that is similar to that found for the af-/reforestation simulation. The response times of total land C pools to the drastic land cover and land management changes lie within a period of 160 years, since only very small changes can be detected at the end of the simulation period. These results suggest the need to avoid cropland expansion, not only due to the local loss of total C (not shown), but also due to the higher unintended loss of total land C compared to af-/reforestation, induced by unfavorable remote climate effects.

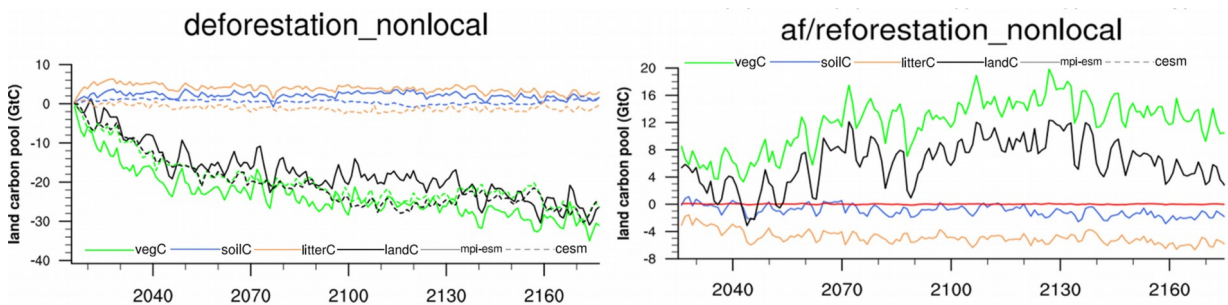


Figure 3: Global unintended effects of cropland expansion (deforestation, left) and af-/reforestation (right) on vegetation C, soil C, litter C for MPI-ESM and CESM

Even on the long-term, highest unintended effects on C pools are simulated for C stored in the vegetation and much less (and with opposite sign) for litter and soil C (Fig. 3). Cropland expansion leads to a negative impact on vegetation C but a positive impact on litter and soil C, whereas for af-/reforestation the sign of change is reversed. However, the relative contribution of litter and soil C to the total land C is higher for unintended effects due to af-/reforestation than for cropland expansion.

The regional pattern of the effects on vegetation C due to cropland expansion are simulated similarly for MPI-ESM and CESM (Fig. 4). There are differences in the boreal region (CESM simulates stronger decrease in vegetation C) and the Congo region (MPI-ESM simulates stronger decrease in vegetation C) which can be related to differences in nonlocal 2m air temperature and precipitation. Generally, the unintended vegetation C decrease in the Amazon region and the Congo region is accompanied by 2m air temperature increase and precipitation decrease for both models. Whether the

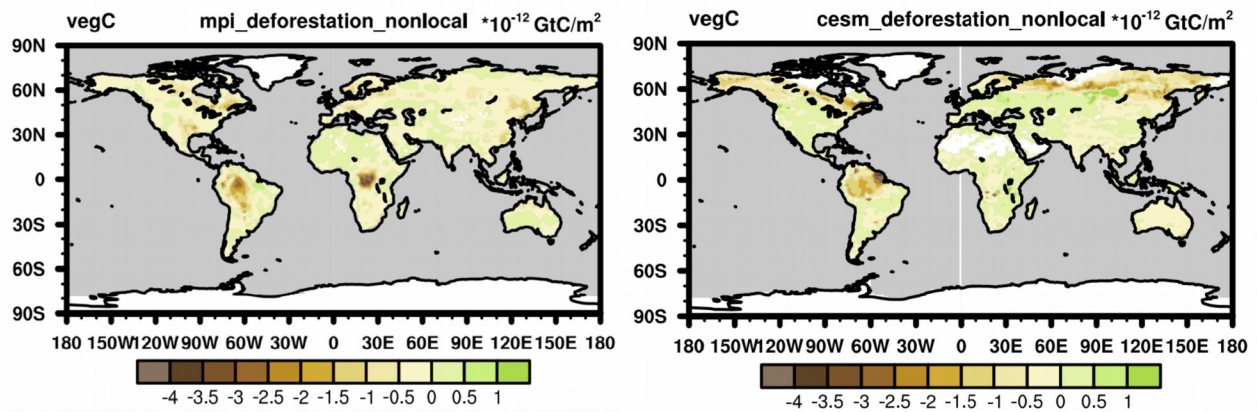


Figure 4: Spatial distributed unintended effects of cropland expansion on vegetation C simulated by MPI-ESM-1.2 (left) and CESM (right)

tropical vegetation becomes heat stressed still needs to be analyzed.

The extent of land cover and land management change certainly determines the magnitude of unintended C cycle changes. Here, we performed global land cover and land management changes on 50% of all grid points, which is used to differentiate the sensitivity of the signals. However, the absolute impact on the different C pools cannot be translated directly to real world land-based climate mitigation measures.

4. Heat impact on labor productivity in India

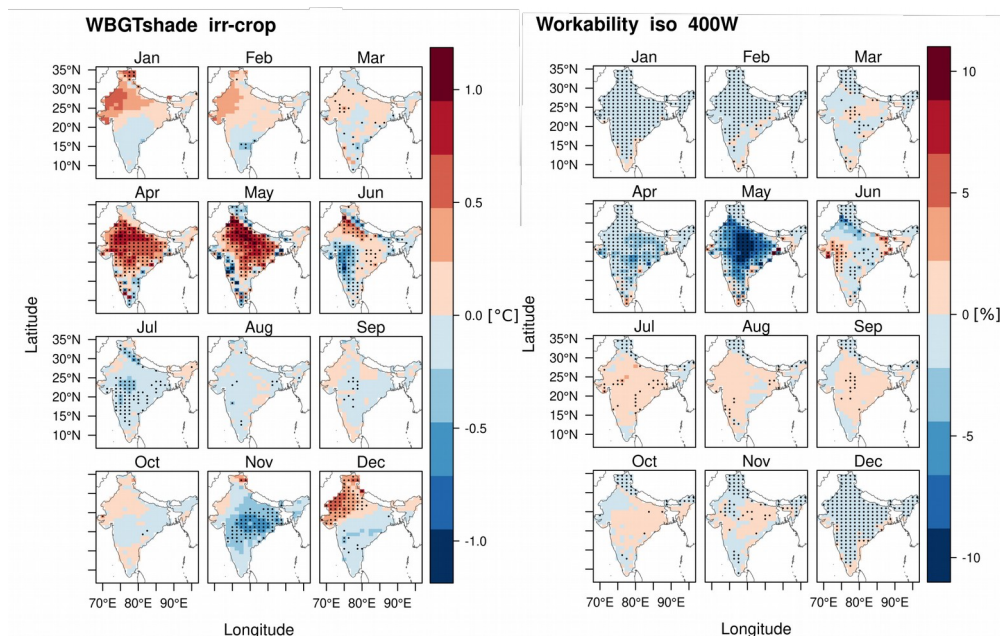


Figure 5: Impact of irrigation on wet bulb globe temperature [°C] for shaded conditions (WBGTshade) (left), and resulting change of labor productivity [%] (right) in India based on CESM sensitivity experiments.

All ESM output was stored on /arch and additionally used to study the impact on worker productivity of irrigated cropland expansion compared to rainfed cropland expansion, which is why these results are shown and briefly described here. Figure 5 shows the calculated wet bulb globe for shaded conditions temperature (WBGT) which is then used

to derive the heat effects on worker productivity (calculated by NIOSH/ISO heat assessment metric under high-intensity work (400 W)) which will be implemented in the socio-economic model GRACE in a next step. Especially in April and May, irrigation in India induces a substantial heating effect and thereby leading to a reduction in workability. The global economic responses to heat stress impacts on worker productivity in agriculture are comparable to those on crop yields.

5. Land management-based emulator

ESM output from the idealized experiments stored on /arch was also used to train a climate emulator making use of land cover and land management effects on surface temperature and relative humidity (see Fig. 6).

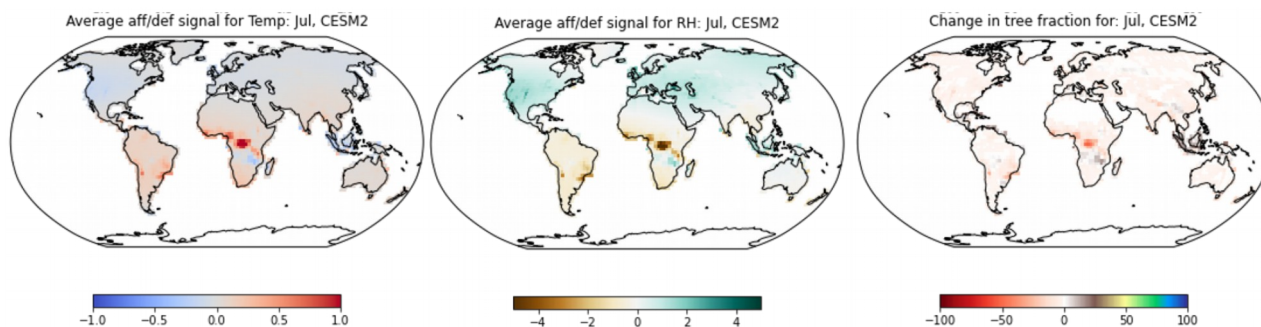


Figure 6: Change of local surface temperature [$^{\circ}\text{C}$] (left) and relative humidity [%] (middle) due to change in tree fraction (right) in July at the end of 21st century

MESMER-LCLM (the land cover land management module of the climate emulator MESMER-M (Nath et al., in prep)) is able to calculate the local signal for surface temperature and surface relative humidity by using end-of-century land forcing from the SSP5-8.5 runs of CESM2. Additionally, a Generalized Additive Model (GAM) was used to represent the land cover and land management signals.